

## ANALYSIS OF MICROBUCKLING FOR MONOMOLECULAR LAYERS ADHERING TO A SUBSTRATE\*

Chang Tienchong (张田忠)<sup>1,3</sup> Guo Wanlin (郭万林)<sup>2,3</sup> Li Guoqiang (李国强)<sup>1</sup>

<sup>1</sup>(College of Civil Engineering, Tongji University, Shanghai 200092, China)

<sup>2</sup>(Department of Aircraft Engineering, Nanjing University of Aeronautics and Astronautics, Nanjing 210016, China)

<sup>3</sup>(State Key Laboratory of Structural Strength and Vibration, Xi'an Jiaotong University, Xi'an 710049, China)

**ABSTRACT:** A two-dimensional linear spring model is established to study the microbuckling of a plane monomolecular layer adhering to a substrate. The model is for the layer subjected to a compressive load having an arbitrary angle with the chemical bond of the layer. The effects of the load angle, the strength of adhesion and the bending stiffness and shearing stiffness (the capability of resisting transverse bending and in-plane shearing) of the layer on the minimal buckling force and the critical buckling mode are discussed. It is found that the minimal buckling force increases with increasing load angle and, for a given bending stiffness, increases with increasing strength of adhesion and decreasing shearing stiffness. Furthermore, a critical condition under which the buckling of the layer can just occur is obtained, which is helpful to avoid buckling in an engineering application.

**KEY WORDS:** nanotechnology, microbuckling, monomolecular layer, spring model

### 1 INTRODUCTION

A thin layer can be formed when one material is coated on the surface of another material for a special purpose, such as, some metal material coated on both sides of silicone film as electrodes of an electrical actuator<sup>[1]</sup>, or amorphous diamond-like-carbon as wear-protective coatings of head-disk interface<sup>[2]</sup>. If the layer fails, it may cease to function and the system may fail too. The performance and reliability of thin films are often closely associated with their mechanical behavior. Therefore, the mechanical behaviors, such as debonding, buckling, sliding, fracture and so on, of thin layers are widely investigated by both theoretical and experimental methods<sup>[1~12]</sup>.

With the development of science and technology, the size of microstructure tends to a molecular scale and a new research subject of so called nanotechnology emerges. Investigation on mechanical behavior of molecularly thin layers is one important branch of

---

Received 1 June 2001, revised 31 December 2001

\* The project supported by the National Distinguished Young Scientist Fund, Cheung Kong Scholars Programme, the National Natural Science Foundation of China (10272082, 10172068) and Shanghai Post-doctoral Science Foundation

nanotechnology. In this branch, owing to the discrete nature of molecular layers, continuum mechanics can not be used<sup>[13]</sup> and some novel methods and new approaches are needed.

One of the most common problem encountered in molecular layers is instability, such as buckling of a carbon nanotube<sup>[13]</sup> or rippling of a collapsing bubble<sup>[14]</sup>. Although a free element method was developed to deal with the instability problem of micromachined beams<sup>[15]</sup>, as pointed out by Chisks and Parnes<sup>[16]</sup>, the more corrugated buckling mode of an element which is not free but interacts with others is considerably different from that of the free element. Therefore, Chisks and Parnes<sup>[16]</sup> presented a linear spring model, in which inextensible chain segments interact with each other by means of spiral springs and with the substrate by means of usual springs, to simulate the buckling of monomolecular layers adhering to a substrate. However, this model is limited to a one-dimensional simulation, that is, it can only consider the effects of the resistance of the layer to transverse bending but not to in-plane shearing. In fact, the in-plane shearing has a quite significant effect on the buckling behavior, as can be seen in the following sections. Furthermore, the one-dimensional model can only deal with the case of the layer subjected to the compressive load along the chemical bonds. Recently, Chang et al.<sup>[17]</sup> extended the one-dimensional model to a special two-dimensional case when the compressive load has an angle of  $\pi/4$  with the chemical bonds. Still, this two-dimensional model cannot handle the more general case under a compressive load having an arbitrary angle.

In this paper, a linear spring model is developed to demonstrate the buckling behavior of a monomolecular layer subjected to a compressive load having an arbitrary angle with the chemical bonds. The layer is modeled as a lattice network in which each node represents a molecule or an atom. The resistance of the layer to out-of-plane transverse bending and to in-plane shearing is simulated by spiral springs and the adhesion stiffness is simulated by usual springs. The effects of bending stiffness and shearing stiffness of the layer on the critical buckling force and the buckling mode are analyzed in detail.

## 2 THE LINEAR SPRING MODEL

We consider a monomolecular layer of molecules or atoms spaced a distance  $a$  apart glued to a substrate, as shown in Fig.1. The layer is modeled as a lattice network. Each node of the network corresponds to a molecule (or an atom) and the distance between two nodes keeps unchanged. The layer, assumed to be connected to the substrate by means of linear springs, is subjected to a compressive load,  $F$ , with a line density of  $f$ . The interactions between two molecular bonds are modeled by means of spiral springs. Such springs represent the angular forces resulting from the adjustment of the electron clouds

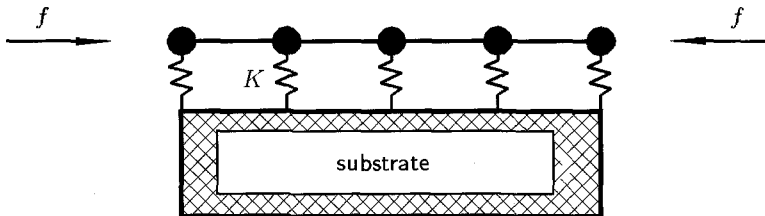


Fig.1 Spring model of the problem. The linear spring  $K$  is used to model the adhesion between the layer and the substrate, while the spiral springs are used to model the angular forces of the adjustment of the electron clouds surrounding the molecules

surrounding the molecules. It can be expected that there need two spiral springs to simulate the angular forces, one for transverse bending and the other for in-plane shearing, because the density of the electron clouds is different in the transverse section and in the plane of the layer.

The potential energy  $U$  of a spiral spring with an angular displacement of  $\varphi$  can be shown as

$$U = \frac{C}{2}\varphi^2 \quad (1)$$

and the potential energy  $V$  of a linear spring with an extension  $q$  is

$$V = \frac{K}{2}q^2 \quad (2)$$

wherein  $C$  and  $K$  are the elastic rigidities of the two springs, respectively.

The work of the applied load,  $F$ , on a displacement  $\delta$ , is calculated as

$$W = F\delta \quad (3)$$

Then, the free energy of the system can be written as

$$\Pi = U + V - W \quad (4)$$

With the conditions of the extremum of the principle of the minimal energy, we can obtain the relationship between the buckling force and the buckling mode.

### 3 BASIC EQUATIONS

When the applied compressive load  $F$ (or  $f$ ) has an angel  $\beta$  with the chemical bond (as shown in Fig.2(a)), we can assume that  $F$ (or  $f$ ) is along the line through nodes  $ij$  and  $(i+m)(j-n)$ . That is, load angle  $\beta$  can be determined by

$$\tan \beta = \frac{n}{m} \quad (5)$$

where  $m$ ,  $n$  are relative prime numbers.

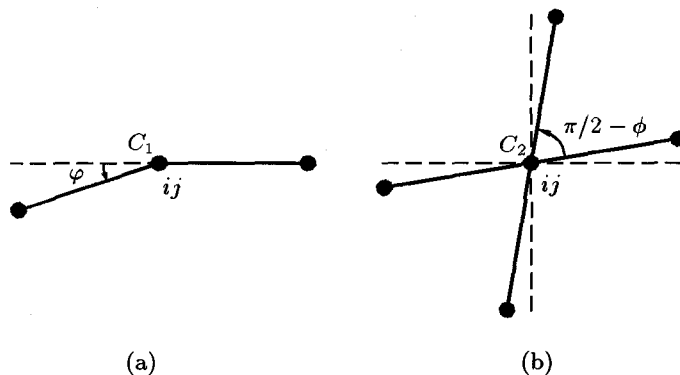


Fig.2 Transverse buckling (a) and in-plane shear deformation (b) of the layer. The rigidities of the spiral springs modeling the angular forces of the adjustment of the electron clouds surrounding the molecules are  $C_1$  and  $C_2$ , and the elastic energies are  $C_1\varphi^2/2$  and  $C_2\phi^2$ , respectively

In the transverse direction, spiral spring  $C_1$  (with elastic rigidities of  $C_1$ ) is used to simulate the angular forces resulting from the adjustment of the electron clouds surrounding node  $ij$ , and the angular deformations (Fig.3(a)) in two directions ( $i$  and  $j$ ) are

$$\varphi_{ij1} = \zeta_{(i+1)j} - 2\zeta_{ij} + \zeta_{(i-1)j} \tag{6}$$

$$\varphi_{ij2} = \zeta_{i(j+1)} - 2\zeta_{ij} + \zeta_{i(j-1)} \tag{7}$$

where,  $\zeta_{ij}$  is the displacement of node  $ij$  in transverse direction normalized by  $a$ .

Similarly, the in-plane interaction between two chemical bonds can be simulated by spiral spring  $C_2$  (with elastic stiffness of  $C_2$ ) and the angular deformation is (see Fig.3(b))

$$\phi_{ij} = \frac{\delta'}{m} + \frac{\delta'}{n} \tag{8}$$

where

$$\delta' = \frac{\kappa f a^2 m^2 n^2}{2C_2(m+n)^2} \tag{9}$$

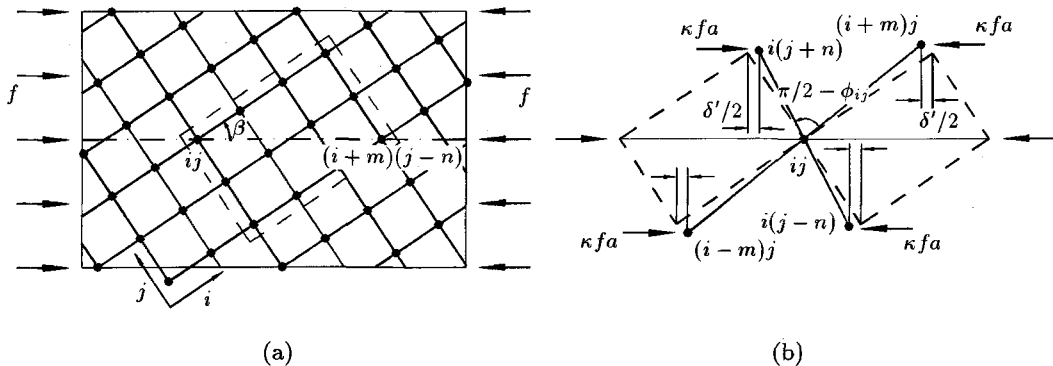


Fig.3 Applied compressive force has an angel of  $\beta$  with the chemical bond of the layer (a); in-plane shear deformation near node  $ij$  (b)

Then the energy  $U$ ,  $V$  and the work  $W$  can be written as

$$U_{ij} = \frac{1}{2}C_1(\varphi_{ij1}^2 + \varphi_{ij2}^2) + C_2\phi_{ij}^2 = \frac{1}{2}C_1(\zeta_{(i+1)j} - 2\zeta_{ij} + \zeta_{(i-1)j})^2 + \frac{1}{2}C_1(\zeta_{i(j+1)} - 2\zeta_{ij} + \zeta_{i(j-1)})^2 + \frac{m^2 + n^2}{m^2 n^2} C_2 \delta'^2 \tag{10}$$

$$V_{ij} = \frac{K}{2}q_{ij}^2 = \frac{1}{2}K a^2 \zeta_{ij}^2 \tag{11}$$

$$W_{ij} = \kappa f a^2 \delta_{ij} \tag{12}$$

where

$$\kappa = \frac{1}{\sqrt{m^2 + n^2}} \tag{13}$$

$$\delta_{ij} = \sqrt{P^2 + Q^2 - 2PQ \sin \phi_{ij}} \tag{14}$$

in which

$$P = \sum_{k=1}^m \left\{ \sqrt{1 - (\zeta_{(i+k)j} - \zeta_{(i+k-1)j})^2} \right\} \quad Q = \sum_{k=1}^n \left\{ \sqrt{1 - (\zeta_{i(j-k+1)} - \zeta_{(i-k)j})^2} \right\} \quad (15)$$

For relatively small  $\zeta_{ij}$

$$P = m - \frac{1}{2} \sum_{k=1}^m \left\{ (\zeta_{(i+k)j} - \zeta_{(i+k-1)j})^2 \right\} \quad Q = n - \frac{1}{2} \sum_{k=1}^n \left\{ (\zeta_{i(j-k+1)} - \zeta_{(i-k)j})^2 \right\} \quad (16)$$

$$\delta_{ij} = \left[ m^2 - \left( m - \left( 1 + \frac{n}{m} \right) \delta' \right) \sum_{k=1}^m \left\{ (\zeta_{(i+k)j} - \zeta_{(i+k-1)j})^2 \right\} + n^2 - \left( n - \left( 1 + \frac{m}{n} \right) \delta' \right) \sum_{k=1}^n \left\{ (\zeta_{i(j-k+1)} - \zeta_{(i-k)j})^2 \right\} - 2(m+n)\delta' \right]^{1/2} \quad (17)$$

The free energy of node  $ij$  can then be expressed as

$$\Pi_{ij} = U_{ij} + V_{ij} - W_{ij} \quad (18)$$

Conditions of extremum of the free energy of the system yield

$$\frac{\partial \Pi}{\partial \zeta_{ij}} = \frac{\partial}{\partial \zeta_{ij}} \sum \{ U_{ij} + V_{ij} - W_{ij} \} = 0 \quad (19)$$

that is

$$C_1 \left( D_i^{(4)} + D_j^{(4)} \right) \zeta_{ij} + K a^2 \zeta_{ij} + \kappa f a^2 D \zeta_{ij} = 0 \quad (20)$$

in which the operators are defined as

$$D \zeta_{ij} = \frac{\partial \delta_{ij}}{\partial \zeta_{ij}} = \frac{1}{\delta_{ij}} \left[ (m^2 - (m+n)\delta') D_i^{(2)} \zeta_{ij} + (n^2 - (m+n)\delta') D_j^{(2)} \zeta_{ij} \right] \approx \frac{1}{\sqrt{m^2 + n^2}} \left[ (m^2 - (m+n)\delta') D_i^{(2)} \zeta_{ij} + (n^2 - (m+n)\delta') D_j^{(2)} \zeta_{ij} \right] \quad (21)$$

$$D_i^{(4)} = D_i^{(2)} \zeta_{(i+1)j} - 2D_i^{(2)} \zeta_{ij} + D_i^{(2)} \zeta_{(i-1)j} \quad (22)$$

$$D_j^{(4)} = D_j^{(2)} \zeta_{i(j+1)} - 2D_j^{(2)} \zeta_{ij} + D_j^{(2)} \zeta_{i(j-1)} \quad (23)$$

where

$$D_i^{(2)} \zeta_{ij} = \zeta_{(i+1)j} - 2\zeta_{ij} + \zeta_{(i-1)j} \quad (24)$$

$$D_j^{(2)} \zeta_{ij} = \zeta_{i(j+1)} - 2\zeta_{ij} + \zeta_{i(j-1)} \quad (25)$$

The following buckling mode is sought for the problem

$$\zeta_{ij} = Z \cos \left[ \left( i - \frac{n}{m} j \right) \frac{\pi}{N} \right] \quad N = 1, 2, 3, \dots \quad (26)$$

where  $N$  is the numbers of molecules in a half-period of buckling shapes. Note that the buckling modes corresponding to  $N = 1$  and  $N = 2$  are saw-like shapes which are so called nanobuckling where the neighboring molecules are shifted in the antiphase.

Using buckling mode Eq.(26), the operators can be written as

$$D\zeta_{ij} = \frac{-4}{\sqrt{m^2 + n^2}} \left[ (m^2 - (m+n)\delta') \sin^2 \frac{\pi}{2N} + (n^2 - (m+n)\delta') \sin^2 \frac{n\pi}{2mN} \right] \zeta_{ij} \quad (27)$$

$$D_i^{(2)}\zeta_{ij} = -4 \sin^2 \frac{\pi}{2N} \zeta_{ij} \quad (28)$$

$$D_i^{(4)} = 16 \sin^4 \frac{\pi}{2N} \zeta_{ij} \quad (29)$$

$$D_j^{(2)}\zeta_{ij} = -4 \sin^2 \frac{n\pi}{2mN} \zeta_{ij} \quad (30)$$

$$D_j^{(4)} = 16 \sin^4 \frac{n\pi}{2mN} \zeta_{ij} \quad (31)$$

Substituting the above expressions of the operators into Eq.(20) leads to

$$\begin{aligned} \kappa f a^2 \frac{-4}{\sqrt{m^2 + n^2}} \left[ (m^2 - (m+n)\delta') \sin^2 \frac{\pi}{2N} + (n^2 - (m+n)\delta') \sin^2 \frac{n\pi}{2mN} \right] \zeta_{ij} + \\ C_1 \left( 16 \sin^4 \frac{\pi}{2N} \zeta_{ij} + 16 \sin^4 \frac{n\pi}{2mN} \zeta_{ij} \right) + K a^2 \zeta_{ij} = 0 \end{aligned} \quad (32)$$

The characteristic equation can then be obtained, for nontrivial solution  $\zeta_{ij} \neq 0$ , as

$$\begin{aligned} \kappa^3 f^2 a^4 \frac{m^2 n^2}{2C_2(m+n)} \left( \sin^2 \frac{\pi}{2N} + \sin^2 \frac{n\pi}{2mN} \right) - 4\kappa^2 f a^2 \left( m^2 \sin^2 \frac{\pi}{2N} + n^2 \sin^2 \frac{n\pi}{2mN} \right) + \\ C_1 \left( 16 \sin^4 \frac{\pi}{2N} + 16 \sin^4 \frac{n\pi}{2mN} \right) + K a^2 = 0 \end{aligned} \quad (33)$$

Let

$$A_1 = \frac{\kappa^3 m^2 n^2 S}{2(m+n)} \left( \sin^2 \frac{\pi}{2N} + \sin^2 \frac{n\pi}{2mN} \right) \quad (34)$$

$$A_2 = -4\kappa^2 \left( m^2 \sin^2 \frac{\pi}{2N} + n^2 \sin^2 \frac{n\pi}{2mN} \right) \quad (35)$$

$$A_3 = \left( 16 \sin^4 \frac{\pi}{2N} + 16 \sin^4 \frac{n\pi}{2mN} \right) + R \quad (36)$$

where

$$S = C_1/C_2 \quad R = K a^2/C_1 \quad (37)$$

Using the above parameters  $A_1$ ,  $A_2$  and  $A_3$ , the characteristic equation can be simplified as

$$A_1 \left( \frac{f}{C_1/a^2} \right)^2 + A_2 \frac{f}{C_1/a^2} + A_3 = 0 \quad (38)$$

and hence the buckling force  $f_b$ , normalized by  $(C_1/a^2)$  is given by

$$\frac{f_b}{C_1/a^2} = \frac{-A_2 - \sqrt{A_2^2 - 4A_1A_3}}{2A_1} \quad (39)$$

#### 4 DISCUSSIONS ON THE MINIMAL BUCKLING FORCE AND THE CRITICAL BUCKLING MODE

It can be seen from Eq.(39) that the buckling force  $f_b$  depends on the buckling mode  $N$ , and is affected by the force angle  $\beta$  (i.e.  $m$  and  $n$ ) and two parameters  $S$  and  $R$ . In an engineering application, the most important is the minimal buckling force (critical buckling force). To find the critical buckling mode  $N_c$  to which the minimal buckling force corresponds, the effects of the parameters  $m$  and  $n$ ,  $S$  and  $R$  should be discussed firstly.

##### 4.1 Effects of $m$ and $n$

Figure 4 shows the variation of the normalized buckling force  $f_b/(C_1 \cdot a^{-2})$  versus  $N$  for difference  $n : m$  when  $R = 8$  and  $S = 0.01$ . The figure shows that the minimal buckling force  $f_b$  increases with the increase of  $\beta$  (or  $n : m$ ). It is also seen that the critical  $N_c$  to which the minimal buckling force corresponds shows a tendency of getting smaller. So the following relation can be obtained reasonably

$$N_c(0 : 1; R; S) \leq N_c(n : m; R; S) \leq N_c(1 : 1; R; S) \tag{40}$$

where  $N_c(n : m; R; S)$  represents  $N_c$  as a function of  $n : m$  (or  $\beta$ ),  $R$  and  $S$ . It should be noticed that  $N_c$  is an integer number in real problems, so the actual minimal buckling force is not the lowest point of the curves shown in Fig.4 but the value corresponding to  $N_c$ .

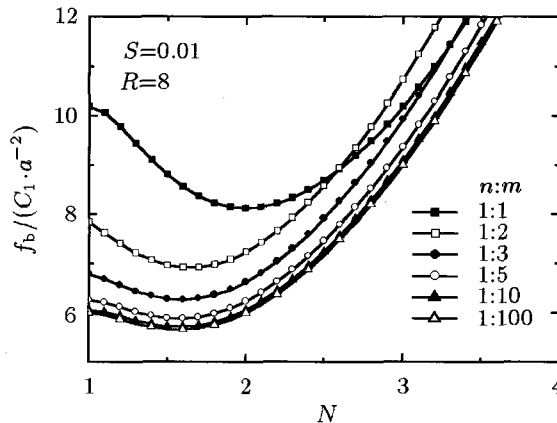


Fig.4 Effect of  $n : m(\beta)$  on nondimensional  $f_b$ - $N$  behavior for  $S = 0.01$  and  $R = 8$

##### 4.2 Effects of $R$

Figure 5 shows the buckling force  $f_b$  as a function of  $N$  for a series of  $R$  values when  $n : m = 1 : 3$  and  $S = 0.1$ . It can be seen that the minimal buckling force increases with the increase of  $R$ , while  $N_c$  shows a tendency towards a smaller one. That is

$$N_c(n : m; R_1; S) \geq N_c(n : m; R_2; S) \quad \text{if } R_1 < R_2 \tag{41}$$

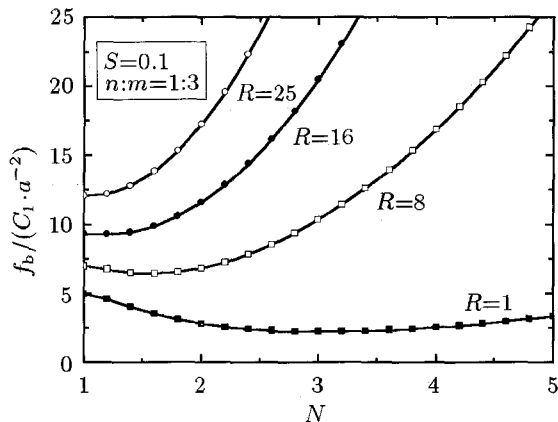


Fig.5 Effect of  $R$  on nondimensional  $f_b$ - $N$  behavior for  $S = 0.1$  and  $n : m = 1 : 3$

4.3 Effects of  $S$

The effect of  $S$  on the buckling force  $f_b$  is shown in Fig.6, where  $R = 8$  and  $n : m = 1 : 3$ . The figure shows that the minimal buckling force increases with increasing  $S$ . One is surprised to see, however, that  $S$  only shows little influence on  $N_c$ . To check if it is only a special case shown in Fig.6, Fig.7 with  $R = 1$  and  $n : m = 1 : 3$  is added to re-confirm the conclusion. Again,  $S$  has little effect on  $N_c$ . This is a very important conclusion because the procedure of determining the approximate value of  $N_c$  for arbitrary  $S$  can be simplified with the assumption of  $S = 0$ . The specific procedure will be shown in Section 6.

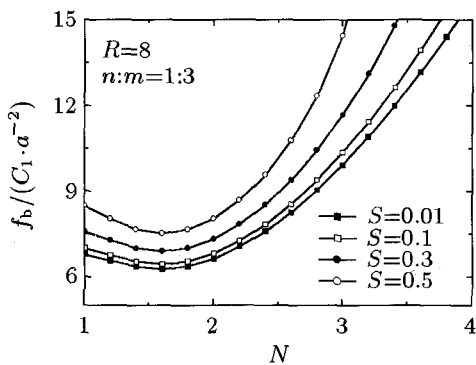


Fig.6 Effect of  $S$  on nondimensional  $f_b$ - $N$  behavior for  $R = 8$  and  $n : m = 1 : 3$

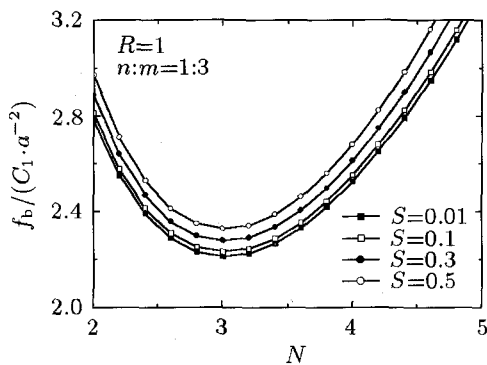


Fig.7 Effect of  $S$  on nondimensional  $f_b$ - $N$  behavior for  $R = 1$  and  $n : m = 1 : 3$

5 TYPICAL CASES FOR  $S = 0$

$S = 0$  (i.e.  $C_2 \gg C_1$ ) stands for a very high ability of the monolayer to resist shear deformation (or there is even no in-plane shear deformation).

5.1  $n : m = 0 : 1$  (or  $\beta = 0$ )

When  $n : m = 0 : 1$ , that is, the compressive load is applied along the chemical bond



direction, the expression of the buckling force can be simplified as

$$\frac{f_b}{C_1/a^2} = 4\mu + \frac{R}{4\mu} \quad \mu = \sin^2 \frac{\pi}{2N} \quad (42)$$

This result is the same as the one given by Chicks and Parnes<sup>[16]</sup> in one-dimensional model. This shows that the present two-dimensional model degenerates to the one-dimensional model when  $\beta = 0$ . The minimal buckling mode can be determined by the following procedure in this case.

1) If  $R > 16$ ,  $N_c = 1$ ;

2) When  $R \leq 16$ , let  $N_* = \frac{\pi/2}{\arcsin(R^{1/4}/2)}$ , then,

If  $R > 16 \sin^2 \frac{\pi}{2[N_*]} \sin^2 \frac{\pi}{2[N_* + 1]}$ ,  $N_c = N_*$ ;

If  $R < 16 \sin^2 \frac{\pi}{2[N_*]} \sin^2 \frac{\pi}{2[N_* + 1]}$ ,  $N_c = N_* + 1$ ,

where  $[N_*]$  represents the maximum integer less than  $N_*$ .

It is easy to obtain from the above equations that the buckling mode will have a saw shape ( $N = 1$ ) for  $R > 8$  and a saw shape ( $N = 2$ ) for  $2 < R < 8$  (see Fig.8). Both phenomena in which the neighboring molecules along the  $i$  direction are shifted in the antiphase are called nanobuckling<sup>[16]</sup>.

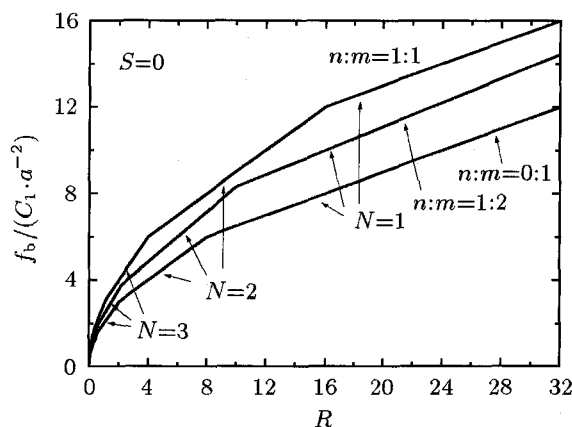


Fig.8 Minimal buckling forces as function of  $R$  showing corresponding buckling modes for different ( $\beta$ )  $n : m$  when  $S = 0$

### 5.2 $n : m = 1 : 1$ (or $\beta = \pi/4$ )

$n : m = 1 : 1$  means the compressive force is applied along the bisector of the angle between the chemical bonds perpendicular to each other. The buckling force is given by

$$\frac{f_b}{C_1/a^2} = 8\mu + \frac{R}{4\mu} \quad \mu = \sin^2 \frac{\pi}{2N} \quad (43)$$

The expression of the buckling force is similar to the case of  $\beta = 0$ , so the procedure to determine  $N_c$  is similar too:

1) If  $R > 32$ ,  $N_c = 1$ ;

2) When  $R \leq 32$ , let  $N_* = \frac{\pi/2}{\arcsin(R/32)^{1/4}}$ , then,

$$\text{If } R > 32 \sin^2 \frac{\pi}{2[N_*]} \sin^2 \frac{\pi}{2[N_* + 1]}, N_c = N_*;$$

$$\text{If } R < 32 \sin^2 \frac{\pi}{[N_*]} \sin^2 \frac{\pi}{[N_* + 1]}, N_c = N_* + 1,$$

where  $[N_*]$  represents the maximum integer less than  $N_*$ .

In this case, nanobuckling occurs when  $R > 4$ ,  $4 < R < 16$  for  $N = 2$  and  $R > 16$  for  $N = 1$  (Fig.8).

### 5.3 Arbitrary $n : m$

For an arbitrary ratio of  $n : m$ , the buckling force can be written as

$$\frac{f_b}{C_1/a^2} = \frac{(m^2 + n^2) [16(\mu^2 + \lambda^2) + R]}{4(m^2\mu + n^2\lambda)} \quad \mu = \sin^2 \frac{\pi}{2N} \quad \lambda = \sin^2 \frac{n\pi}{2mN} \quad (44)$$

It is known from Eq.(40) in Section 4 that

$$N_c(0 : 1; R; 0) \leq N_c(n : m; R; 0) \leq N_c(1 : 1; R; 0) \quad (45)$$

To determine the critical minimal buckling mode  $N_c$ , one need check all of the integers between  $N_c(0 : 1; R; 0)$  and  $N_c(1 : 1; R; 0)$  to find to which  $N$  the minimal buckling force corresponds.

Together with the discussion in Sections 3.1 and 3.2, we know that

$$N_c(n : m; R; 0) = 1, \text{ if } R > 16$$

$$N_c(n : m; R; 0) = 1 \text{ or } 2, \text{ if } 8 < R < 16$$

$$N_c(n : m; R; 0) = 2, \text{ if } 4 < R < 8$$

$$N_c(n : m; R; 0) = 2 \text{ or } 3, \text{ if } 2 < R < 4$$

...

A typical case of  $n : m = 1 : 2$  is also shown in Fig.8. It can be seen that the curve with  $n : m = 1 : 2$  falls between the curves with  $n : m = 1 : 1$  and  $n : m = 0 : 1$ .

Figure 8 also indicates that when  $S = 0$ , the critical buckling force  $f_{cb}$  is a piece-wise linear incremental function of  $R$ .

## 6 GENERAL CASES

When  $S \neq 0$  and  $\beta \neq 0$ , the minimal buckling force  $f_{cb}$  and  $N_c$  can not be determined directly. It is known, however, from the Section 4.3 that  $S$  has little influence on  $N_c$ , so one can choose  $N_c(n : m; R; 0)$  as an approximate value of  $N_c(n : m; R; S)$  (for  $S \neq 0$ ) under the same conditions at first. Then comparing the buckling force  $f_b$  corresponding to  $N_c(n : m; R; 0)$  and  $N_c(n : m; R; 0) + 1$ , the minimal one should be the critical buckling force  $f_{cb}$  and  $N_c$  is determined at the same time. The procedure of determining  $N_c$  is as follows:

1) Calculate  $N_c(n : m; R; 0)$ ;

2) If  $f_b|_{N_c(n:m;R;0)} < f_b|_{N_c(n:m;R;0)+1}$ ,  $N_c = N_c(n : m; R; 0)$ ; If  $f_b|_{N_c(n:m;R;0)} \geq f_b|_{N_c(n:m;R;0)+1}$ ,  $N_c = N_c(n : m; R; 0) + 1$ .

Another way to determine  $N_c$  is to solve the equation  $f_b|_N = f_b|_{N+1}$  about  $R$  for given  $n : m$  and  $S$  from  $N = 1$  to a relatively large  $N$ . We denote the solution as  $R_N$ . Then

compare  $R$  with all of the  $R_N$ . If the value of  $R$  falls between  $R_N$  and  $R_{N+1}$ ,  $N_c$  should be equal to this  $N$ . That is

$$\text{If } R_N \leq R < R_{N+1}, N_c = N$$

The typical results for  $n : m = 1 : 2$  is shown in Table 1. It is shown that the maximum error between  $R_c$  for different  $S$  is less than 7.5% when  $n : m = 1 : 2$ . It is also found that this error decreases with increasing  $N_c$ .

**Table 1 The critical  $R_c$  for different  $S$  when  $n : m = 1 : 2$**

	$N_c$	7*	6	5	4	3	2	1
$S = 0$	0.032 08	0.056 49	0.109 02	0.238 68	0.626 83	2.161 76	9.935 94	...**
$S = 0.01$	0.032 08	0.056 49	0.109 02	0.238 69	0.626 85	2.162 05	9.958 12	...
$S = 0.1$	0.032 08	0.056 49	0.109 03	0.238 71	0.627 03	2.164 95	10.204 6	...
$S = 0.2$	0.032 08	0.056 49	0.109 03	0.238 74	0.627 24	2.168 68	10.680 1	...
$S = 0.5$	0.032 08	0.056 50	0.109 05	0.238 82	0.627 99	2.186 21	...	...

\* means  $0.032\,08 < R_c < 0.056\,49$  for  $S = 0$ ,  $N_c = 7$ , the rest may be deduced by analogy,

\*\* means  $R_c > 9.935\,94$  for  $S = 0$ ,  $N_c = 1$

Figure 9 shows the minimal buckling force  $f_{cb}$  as a function of  $R$  for different  $S$  when  $n : m = 1 : 2$ . The figure gives a more credible proof that  $S$  has little effect on  $N_c$ .

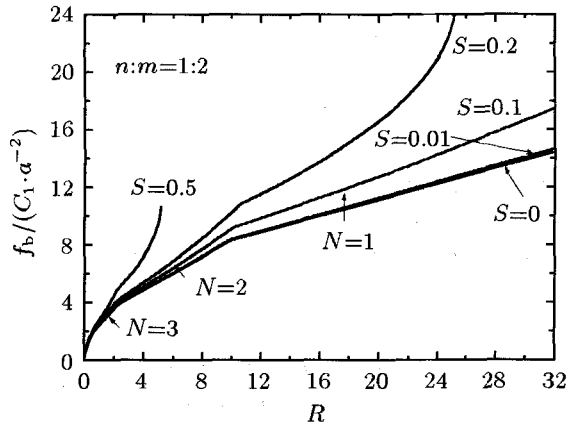


**Fig.9** Minimal buckling forces as function of  $R$  showing corresponding buckling modes for different  $S$  when  $n : m = 1 : 2$

**7 CRITERION OF NO-BUCKLING-OCCURRENCE**

We can see from Fig.9 that the buckling force may not exist under certain  $S$  (for example  $S = 0.5$ ). This indicates that the buckling can be avoided in a monomolecular layer by selecting materials with suitable parameters  $S$  and  $R$ . The criterion of no-buckling-occurring will be discussed in this section.

From Eq.(39), it can be shown that the condition for no-buckling-occurring is

$$A_2^2 - 4A_1A_3 < 0 \tag{46}$$

that is

$$S > \frac{2(m+n)(m^2\mu + n^2\lambda)^2}{m^2n^2\sqrt{m^2 + n^2}(\mu + \lambda)(16\mu^2 + 16\lambda^2 + R)} \tag{47}$$

where

$$\mu = \sin^2 \frac{\pi}{2N_{\min}} \quad \lambda = \sin^2 \frac{n\pi}{2mN_{\min}} \quad (48)$$

in which  $N_{\min}$  is the smallest value of  $N_c$ .

## 8 CONCLUDING REMARKS

A two-dimensional linear spring model is established to analyze the buckling of the monomolecular layer adhering to a substrate. The conclusions of this paper are:

- (1) The present two-dimensional model can consider both effects of the bending stiffness and shear stiffness of the monomolecular layer. When the load is along the chemical bond direction of the layer, this two-dimensional model degenerates to the one-dimensional model given by Chisks and Parnes.
- (2) The minimal buckling force of the monomolecular layer increases with increasing load angle and, for a given bending stiffness, increases with increasing strength of adhesion and decreasing shearing stiffness.
- (3) The critical buckling mode parameter  $N_c$  increases with increasing force angle and, for a given bending stiffness, increases with decreasing strength of adhesion. The shearing stiffness, however, has little effect on  $N_c$ .
- (4) A critical condition under which the buckling of the layer can just occur is obtained, which is helpful to avoid the buckling in an engineering design.

## REFERENCES

- 1 Pelrine R, Kornbluh R, Pei Q, et al. High-speed electrically actuated elastomers with strain greater than 100%. *Science*, 2000, 287(5454): 836~839
- 2 Sivertsen JM, Wang G, Chen GL, et al. Evaluation of amorphous diamond-like carbon-nitrogen films as wear protective coatings on thin film media and thin film head sliders. *IEEE Magnetics*, 1997, 33(1): 926~931
- 3 Bonner T, Baratoff A. Molecular dynamics study of scanning force microscopy on self-assembled monolayers. *Surf Sci*, 1997, 377(1-3): 1082~1086
- 4 Saint-Jalmes A, Gallet F. Buckling in a solid Langmuir monolayer: light scattering measurements and elastic model. *Eur Phys J B*, 1998, 2(4): 489~494
- 5 Dauskardt R, Lane M, Ma Q, et al. Adhesion and debonding of multi-layer thin film structures. *Eng Fract Mech*, 1998, 61(1): 141~162
- 6 Weiss M, Elmer FJ. Dry friction in the Frenkel-Kontorova-Tomlinson model: static properties. *Phys Rev B*, 1996, 53(11): 7539~7549
- 7 Weiss M, Elmer FJ. Dry friction in the Frenkel-Kontorova-Tomlinson model: dynamical properties. *Z Phys B Con Mat*, 1997, 104(1): 55~69
- 8 Shirani A, Liechti KM. A calibrated fracture process zone model for thin film blistering. *Int J Fracture*, 1998, 93(1-4): 281~314
- 9 Wan KT. Fracture mechanics of a V-peel adhesion test—transition from a bending plate to a stretching membrane. *J Adhesion*, 1999, 70(3-4): 197~207
- 10 Evans AG, Hutchinson JW, Wei Y. Interface adhesion: effects of plasticity and segregation. *Acta Mater*, 1999, 47(15-16): 4093~4113
- 11 Bahr DF, Robach JS, Wright JS, et al. Mechanical deformation of PZT thin films for MEMS applications. *Materials Science & Engineering A: Structural Material: Properties, Microstructure & Processing*, 1999, 259(1): 126~131

- 12 Kim SR, Nairn JA. Fracture mechanics analysis of coating/substrate systems. Part I: Analysis of tensile and bending experiments. *Eng Fract Mech*, 2000, 65(4): 573~593
- 13 Falvo MR, Clay GJ, Taylor RM, et al. Bending and buckling of carbon nanotubes under large strain. *Nature*, 1997, 389(6651): 582~584
- 14 Silveira RD, Chaieb S, Mahadevan L. Rippling instability of a collapsing bubble. *Science*, 2000, 287(5457): 1468~1471
- 15 Fang W, Wickert JA. Post buckling of micromachined beams. *J Micromech Micoeng*, 1994, 4(3): 116~122
- 16 Chisks A, Parnes R. On nanobuckling of monomolecular layers adhering to a substrate. *J Appl Mech*, 1999, 66(1): 51~54
- 17 Chang T, Guo W, Yang Z. Microbuckling for monomolecular layer adhering to a substrate under the compressive force with an angle of  $\pi/4$  to the chemical bond. *Acta Mechanica Sinica*, 2001, 33(3): 326~331 (in Chinese)